JOURNAL OF APPLIED POLYMER SCIENCE VOL. 17, PP. 1639–1650 (1973)

Evaluation of Steady-State Flow Curves from Model Molecular Weight Distributions

J. A. COTE and M. SHIDA, *Chemplex Company, Rolling Meadows, Illinois 60008*

Synopsis

Graessley's theory of entanglement was applied to several model distributions. The distribution functions chosen were such that the differential weight distributions were triangular with respect to a log molecular weight axis. The molecular weight level, breadth of the molecular weight distribution, skewness, and blending of simple distributions were studied in their effect on the steady-state flow curve. The governing factor for the shape of the reduced flow curve was shown to be $\bar{M}_{z+1} \cdot \bar{M}_z / \bar{M}_w^2$. Other general features of the flow curve predicted by Graessley's theory were discussed.

INTRODUCTION

Molecular weight and molecular weight distribution are known to have a profound effect on the steady-state flow curves (viscosity η versus shear rate $\dot{\gamma}$) of polymer systems. Many approaches, both theoretical and empirical, have been used to relate features of the molecular weight distribution with experimental viscosity–shear rate data.[1–7]

It is been found experimentally that a large number of polymer samples having similar-shaped molecular weight distributions can be made to conform to a single flow master curve, provided suitable shift factors (such as the zero-shear viscosity and characteristic shear rate $\dot{\gamma}_0$) are used.[8] On the other hand, a multiplicity of such master curves must be used if the distribution changes, either by broadening or multicomponent blending. It has thus been recognized that the form of the master curve itself depends on the molecular weight distribution. Both η_0 and $\dot{\gamma}_0$ are also known to depend on both molecular weight and molecular weight distribution.[6]

The mechanisms, on a molecular scale, which give rise to non-Newtonian behavior, are still only imperfectly understood. In spite of some observed discrepancies for some polymers,[6] Graessley's entanglement theory predicting the viscosity–shear rate dependence of polydisperse polymers[1] is a plausible approach to understanding the molecular dynamics of such systems. The purpose of this paper is to apply the theory to simple model distributions to determine the effect of molecular weight distribution on steady-state flow curves.

THEORY

Graessley's entanglement theory can be used to calculate a viscosity–shear rate master curve for any given distribution of molecular weights. The curve is given in reduced form, that is, in the form η/η_0 as a function of $\dot{\gamma}\tau_0/2$. Knowledge of η_0 and τ_0 is additionally required to match an experimentally observed η-versus-$\dot{\gamma}$ curve.

Let $P(n)dn$ be the number fraction of polymer chains having lengths between n and $n + dn$. The reduced viscosity η/η_0 is defined in terms of communal averages of certain parameters h and g. Define[1]

$$\bar{h}(\dot{\gamma}) = \int_0^\infty n^2 h(\dot{\gamma},n)P(n)dn \Big/ \int_0^\infty n^2 P(n)dn \tag{1}$$

$$\bar{g}(\dot{\gamma}) = \int_0^\infty n g(\dot{\gamma},n)P(n)dn \Big/ \int_0^\infty n P(n)dn \tag{2}$$

and

$$\bar{g}^{5/2}(\dot{\gamma}) = \int_0^\infty n^{7/2} g^{5/2}(\dot{\gamma},n)\, P(n)dn \Big/ \int_0^\infty n^{7/2}\, P(n)dn, \tag{3}$$

then

$$\eta/\eta_0 = \frac{\bar{h}\cdot\bar{g}^{5/2}}{\bar{g}}. \tag{4}$$

Now

$$g(\dot{\gamma},n) = \frac{2}{\pi}\left[\cot^{-1}\theta + \frac{\theta}{1+\theta^2}\right] \tag{5}$$

$$h(\dot{\gamma},n) = \frac{2}{\pi}\left[\cot^{-1}\theta + \frac{\theta(1-\theta)^2}{(1+\theta^2)^2}\right], \tag{6}$$

and the parameter $\theta(\dot{\gamma},n)$ is implicitly defined by

$$\theta(\dot{\gamma},n) = \left(\frac{\eta}{\eta_0}\right)\cdot\left(\frac{\dot{\gamma}\tau_0}{2}\right)\cdot\left(\frac{\mathrm{n}}{n_w}\right)^2 \frac{h(\dot{\gamma},n)}{h(\dot{\gamma})}. \tag{7}$$

The computer program required to evaluate η/η_0 as a function of $\dot{\gamma}\tau_0/2$ has been described earlier.[2,7]

RESULTS AND DISCUSSION

Reduced flow curves (η/η_0 versus $\dot{\gamma}\tau_0/2$) were computed for model triangular distributions. For ease of visualization, the distributions are taken with an elution volume (V) base and treated as though they were molecular weight distribution curves for linear polymers obtained from gel permeation chromatograph (GPC) data. A calibration curve relating the logarithm of molecular weight and elution volume (similar to that used in our laboratories for linear polyethylene) was used to obtain molecular weight data:

$$\log_{10} M = 5.00 - 0.282\,(V - 28).$$

TABLE I
Molecular Weight Averages

Type	$\bar{M}_n \times 10^4$	$\bar{M}_w \times 10^5$	$\bar{M}_z \times 10^6$	$(\bar{M}_{z+1}) \times 10^6$	$\bar{M}_w/\bar{M}_n$	$\bar{M}_{z+1} \cdot \bar{M}_z/\bar{M}_w^2$
Condition: Variable Mol Wt Level, Constant Breadth						
High Mol Wt	11.3	10.8	4.37	7.34	9.52	27.5
Medium Mol Wt	3.09	2.95	1.19	2.00	9.52	27.5
Low Mol Wt	0.844	0.804	0.325	0.546	9.52	27.5
Condition: Variable Breadth, Constant Peak Mol Wt						
Broad	1.46	6.26	4.24	7.34	42.9	79.5
Medium	3.09	2.95	1.19	2.00	9.52	27.5
Narrow	4.27	2.13	6.45	1.05	4.99	14.9
Condition: Skewed, Constant Width at Base						
Peak 1-Skewed to High Mol Wt	3.55	3.44	1.22	2.01	9.68	20.8
Symmetric	3.09	2.95	1.19	2.00	9.52	27.5
Peak Skewed to Low Mol Wt	2.65	2.57	1.17	2.00	9.68	35.7
Condition: Blends						
50:50 High:Low Mol Wt	2.54	3.59	1.93	3.64	14.1	54.5
20% High Mol Wt	3.84	5.28	1.56	2.16	13.7	12.1
10% High Mol Wt	3.43	4.11	1.43	2.11	12.0	17.8
Base Distr.	3.09	2.95	1.19	2.00	9.52	27.5
10% Low Mol Wt	2.22	2.66	1.19	2.00	12.0	33.6
20% Low Mol Wt	1.73	2.37	1.18	2.00	13.7	42.1

Molecular weight averages obtained using this calibration are summarized in Table I. These averages and the calibration itself should be taken only in a relative sense, as a simulation of a typical polymer system. The use of a different calibration would not alter the essential results of this paper.

The distributions used are plotted in each section below. They were chosen to cover molecular weight level, breadth of molecular weight distribution, asymmetry (skewness) in the distribution, and blends or composite distributions.

Graessley has suggested[2] that the shapes of the reduced flow curves are influenced by a high-moment polydispersity index, such as $\bar{M}_{z+1} \cdot \bar{M}_z/\bar{M}_w^2$. The flow behavior of polyisobutylene solutions[9] has been shown to depend on the high moment molecular weight, $M_{z+1} \cdot M_z/M_w$. Kataoka[10] found a correlation between the eritical shear stress for onset of non-Newtonian flow and the same high-moment molecular weight for poly(dimethylsiloxane). We shall present evidence that the shapes of the reduced flow curves are indeed governed by the high-moment polydispersity index, $\bar{M}_{z+1} \cdot \bar{M}_z/\bar{M}_w^2$.

Effect of Molecular Weight

The three distributions shown in Figure 1 have the same distribution breadth and differ only in molecular weight level. The three distributions

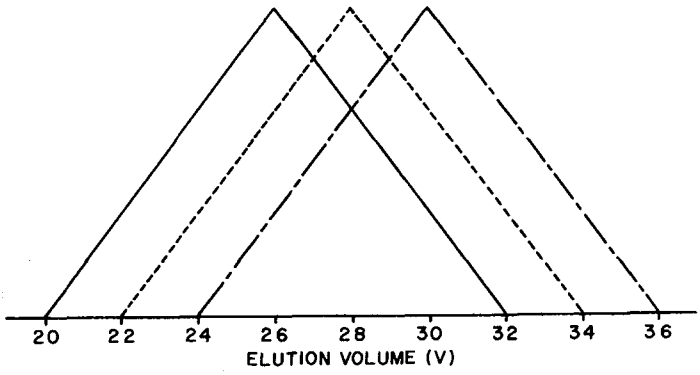

Fig. 1. Distribution functions for molecular weight level effects: (——) high molecular weight; (– – –) medium molecular weight; (——– ·——) low molecular weight.

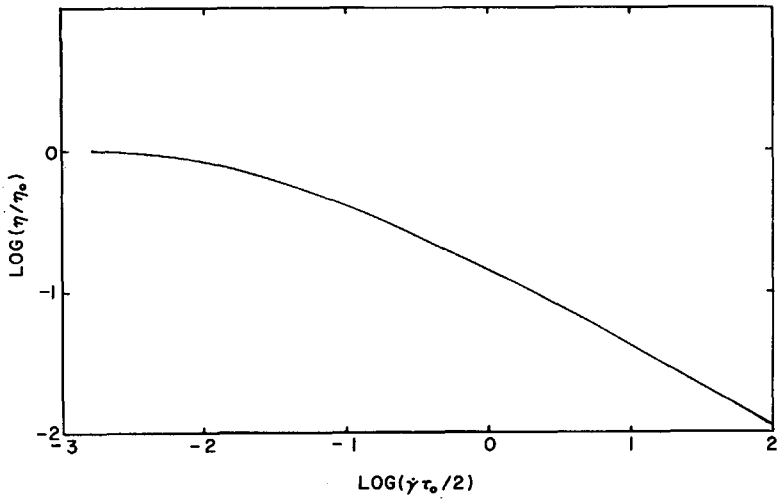

Fig. 2. Flow curve obtained at constant distribution breadth at various molecular weight levels.

give an identical response, namely, a single reduced-flow curve (η/η_0 versus $\dot{\gamma}\tau_0/2$), shown in Figure 2. This apparent independence to molecular weight level predicted by theory has been shown to agree with experimental data[2] for rather narrow ($\bar{M}_w/\bar{M}_n = 1.01$ to 2) molecular weight distribution (MWD) samples.

For resins having a broad MWD, this independence has not been proven experimentally. It is difficult to obtain samples having identical broad MWD and differing only in molecular weight level. The reducing parameters η_0 and τ_0 are both highly molecular weight dependent. The influence of molecular weight level on experimental viscosity–shear rate data is felt through these parameters.

For all three of the model distributions, $\bar{M}_{z+1} \cdot \bar{M}_z/\bar{M}_w^2$ values are, of course, the same.

Effect of Breadth of Molecular Weight Distribution

Figure 3 shows three symmetrical distributions having the same peak molecular weight and differing only in distribution breadth. The polydispersity index $M_{z+1} \cdot M_z / M_w^2$ has a value of 79.5 for the broad distribution, 27.5 for the medium-breadth distribution, and 14.9 for the narrow distribution.

The onset of non-Newtonian flow and the general shape of the reduced flow curves for these three distributions are in agreement with general expectations. These are plotted in Figure 4, along with calculated flow

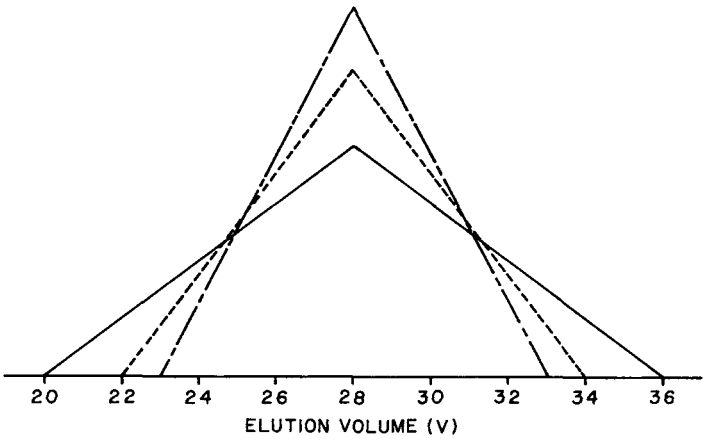

Fig. 3. Distribution functions for effects of breadth of distribution (at constant peak molecular weight): (——) broad distribution; (– – –) medium breadth of distribution; (– — – —) narrow distribution.

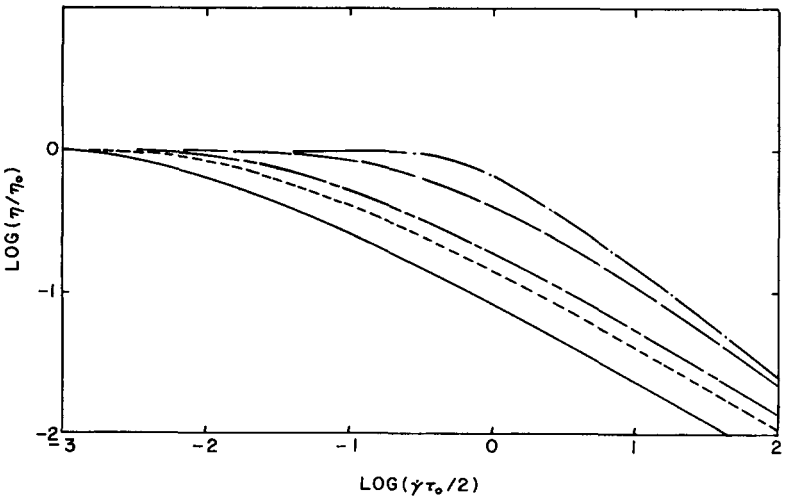

Fig. 4. Flow curves obtained at various breadths of molecular weight distribution: (——) broad; (– – –) medium; (— — — —) narrow; (— — —) most probable distribution; (— · ——) monodisperse case.

curves for monodisperse ($M_w/M_n = 1$) and most probable ($M_w/M_n = 2$, $M_{z+1} \cdot M_z/M_w^2 = 3$) distributions, for comparison. There are two points of interest to note. The first of these is that the effect of MWD on the shape of the flow curve decreases as MWD broadens. The largest changes in the shape of the flow curve take place as we go from the monodisperse case to the most probable distribution case to the narrow distribution. Much greater degrees of broadening are required to achieve similar changes at broad MWD.

The second point is the suggested crossover of flow curves. It is most apparent if the monodisperse flow curve is compared with that for the most probable distribution. To the best of our knowledge, this feature in conjunction with Graessley's theory has not been pointed out in the literature.

We have carried out calculation well beyond the crossover shear rate and found that this is a general feature of the theory, i.e., a narrow MWD flow curve eventually crosses over the flow curve of a broad MWD polymer in the extended shear rate range. Although experimentally it may be difficult to prove this point because of melt instability (e.g., inlet fracture and land fracture[11]) exhibited by polymers, this point should be pursued further.

For the monodisperse distribution, Graessley[1] has shown that the limiting slope at high shear is $-9/11$. The flow curves shown in Figure 4 suggest that the limiting slope for other distributions may be different. An analysis was carried out which shows the limiting slope is $-9/11$ for all distributions. The analysis is given in the Appendix.

Skew Distributions

Figure 5 shows two skew trianglar distributions, one skewed to high molecular weight and one to low molecular weight. These distributions are shown with a symmetrical triangular distribution having the same base. The calculated reduced-flow curves are shown in Figure 6. An interesting feature of these skewed triangular distributions is the fact that M_w/M_n for

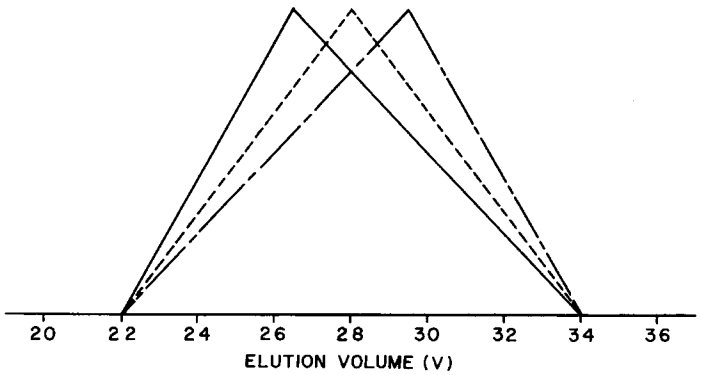

Fig. 5. Skew distribution functions (——) skewed to high molecular weight; (– – –) symmetrical; (—— – ——) skewed to low molecular weight.

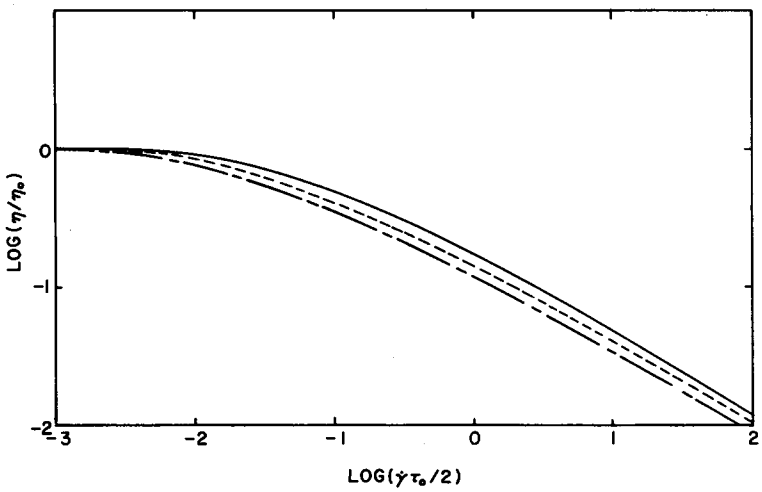

Fig. 6. Flow curves for skew distribution functions: (——) skewed to high molecular weight; (– – –) symmetrical distribution; (——– ——) skewed to low molecular weight.

both are identical, having a value slightly higher than that for the symmetrical distribution. On the other hand, $M_{z+1} \cdot M_z/M_w^2$ increases as we go from the skewed high through the symmetric to the skewed low distribution. A parallel trend can be observed in the shape of the reduced flow curve (Fig. 6), as is observed for the narrow to the broad distribution discussed above.

Composite Distributions

A method of practical importance for modifying distributions is by blending. Figure 7 shows a 50/50 composite distribution of two com-

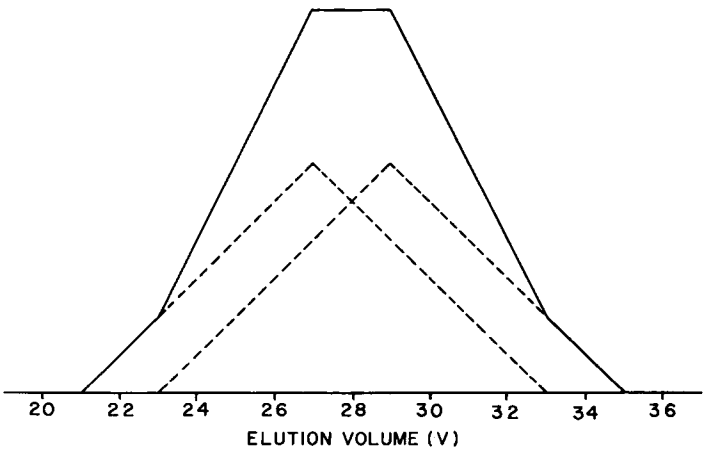

Fig. 7. Distribution function for 50:50 blend of two components having different molecular weight levels, but the same breadth of distribution: (——) blend; (– – –) individual components.

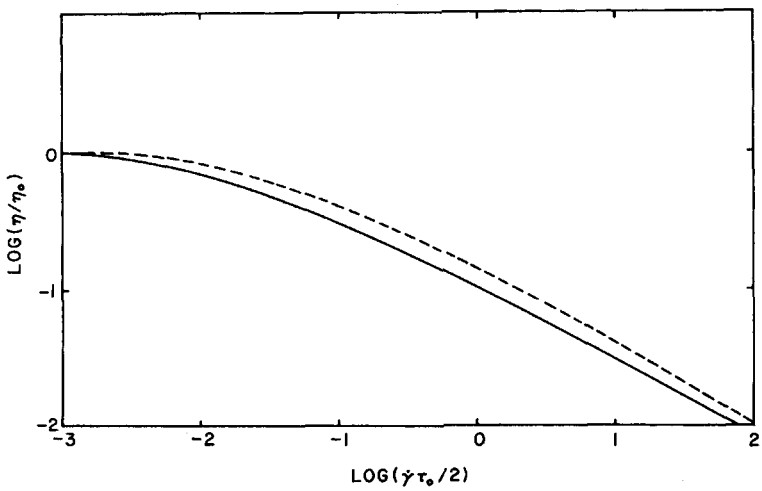

Fig. 8. Flow curve for 50:50 blend: (——) blend; (– – –) components.

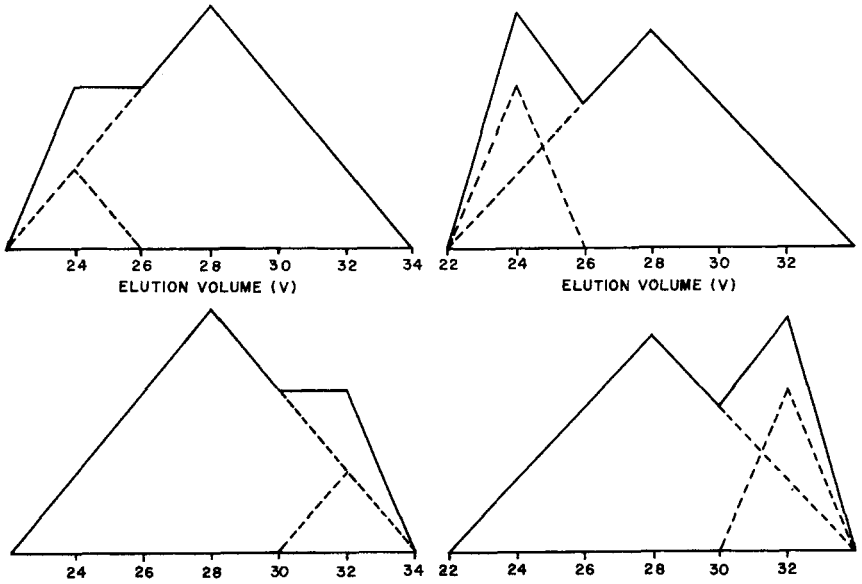

Fig. 9. Distribution functions for blends: (——) blend; (– – –) components; (a) 10% high molecular weight; (b) 20% high molecular weight; (c) 10% low molecular weight; (d) 20% low molecular weight.

ponents having different molecular weight levels with the same breadth MWD. The corresponding reduced-flow curves are shown in Figure 8. The calculated results are as expected.

Figure 9 shows the distributions for several blends. Incorporation of 10% to 20% of high molecular weight components and of 10%, and 20% of low molecular weight components was studied. The reduced-flow curves are shown in Figure 10 for these composite distributions. Here again, the

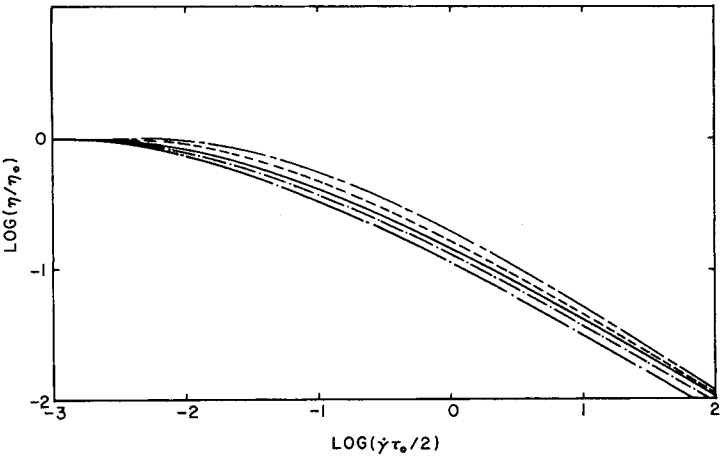

Fig. 10. Flow curves for blends: (——–——) 20% high molecular weight; (– – –) 10% high molecular weight component; (——) unblended parent distribution; (–·–·–·–) 10% low molecular weight component; (—·———·———) 20% low molecular weight component.

shapes of the calculated flow curves are strictly governed by $M_{z+1} \cdot M_z / M_w^2$ and not by M_w/M_n. Experimently, however, almost exactly opposite behavior has been observed by Nakajima and Wong.[6] Their work was carried out using a medium molecular weight linear polyethylene as the base with up to 30% of a high molecular weight or up to 20% of a low molecular weight linear polyethylene added. Their results show that the addition of the high molecular weight component affects the shape of the flow curve in the direction of broader distribution. The addition of the low molecular weight component was shown to have no appreciable effect on the shape of the flow curve. Unfortunately, we do not know any molecular weight averages for their polyethylene samples. Therefore, the values of $M_{z+1} \cdot M_z / M_w^2$ are not known.

CONCLUSIONS

Through use of the model distributions it was shown that the shape of the reduced-flow curve predicted by Graessley's theory is governed by the high-moment polydispersity index, $M_{z+1} \cdot M_z / M_w^2$. The commonly used polydispersity index, M_w/M_n, shows an opposite trend for some cases studied here.

Calculation in the extended shear rate range showed as a general feature of the theory, a crossover of flow curves, and a constant limiting slope of $-9/11$.

Appendix

The equation of the line of limiting slope for polydisperse polymers can be derived as follows:

For large θ, the g and h functions given by eqs. (5) and (6) in the text become, in the limit,

$$g(\dot{\gamma},n) = g(\theta) = \frac{4}{\pi\theta} \tag{1}$$

$$h(\dot{\gamma},n) = h(\theta) = \frac{16}{3\pi\theta^3}. \tag{2}$$

We next take eq. (7) in the text and separate it into an $\eta,\dot{\gamma}$-dependent factor and molecular weight factors

$$\theta(\dot{\gamma},n) = F(\dot{\gamma})\cdot h(\dot{\gamma},n)\cdot\left(\frac{n}{n_w}\right)^2 \tag{3}$$

where

$$F(\dot{\gamma}) = \frac{\eta}{\eta_0}\cdot\frac{\dot{\gamma}\tau_0}{2}\cdot\frac{1}{\bar{h}(\dot{\gamma})} \tag{4}$$

and

$$\bar{h}(\dot{\gamma}) = \frac{\int_0^\infty n^2\cdot h(\dot{\gamma},n)\cdot P(n)dn}{\int_0^\infty n^2\cdot P(n)dn}. \tag{5}$$

Finally, eq. (4) in the text can be written in full:

$$\frac{\eta}{\eta_0} = \frac{\int_0^\infty n^2\cdot h(\dot{\gamma},n)\cdot P(n)dn\cdot\int_0^\infty n^{7/2}g^{5/2}(\dot{\gamma},n)\cdot P(n)dn\cdot\int_0^\infty nP(n)dn}{\int_0^\infty n\cdot g(\dot{\gamma},n)\cdot P(n)dn\cdot\int_0^\infty n^2P(n)dn\cdot\int_0^\infty n^{7/2}P(n)dn}. \tag{6}$$

Eliminating $h(\dot{\gamma},n)$ between eqs. (2) and (3) gives

$$\theta(\dot{\gamma},n) = F(\gamma)\left(\frac{n}{n_w}\right)^2\cdot\frac{16}{3\pi\theta^3(\dot{\gamma},n)} \tag{7}$$

which can be rearranged to give

$$\theta(\dot{\gamma},n) = \left(\frac{16}{3\pi}\right)^{1/4}\left(\frac{n}{n_w}\right)^{1/2}F(\dot{\gamma})^{1/4}. \tag{8}$$

Substituting this expression* for θ into the h term in the expression for h gives

$$\bar{h} = \frac{16}{3\pi}\cdot\frac{\int_0^\infty\frac{n^2}{\theta^3}P(n)dn}{\int_0^\infty n^2P(n)dn} = \left(\frac{16}{3\pi}\right)^{1/4}\cdot\frac{n_w^{3/2}}{[F(\dot{\gamma})]^{3/4}}\cdot\frac{\int_0^\infty n^{1/2}P(n)dn}{\int_0^\infty n^2P(n)dn}. \tag{9}$$

Substituting for $\bar{h}$ in eq. (4) gives

$$F(\dot{\gamma}) = \frac{\eta}{\eta_0}\frac{\dot{\gamma}\tau_0}{2}\cdot\frac{F(\dot{\gamma})^{3/4}}{\left(\frac{16}{3\pi}\right)^{1/4}n_w^{3/2}}\cdot\frac{\int_0^\infty n^2P(n)dn}{\int_0^\infty n^{1/2}P(n)dn} \tag{10}$$

or equivalently

$$F(\dot{\gamma})^{1/4} = \frac{\frac{\eta}{\eta_0}\cdot\frac{\dot{\gamma}\tau_0}{2}\cdot\int_0^\infty n^2P(n)dn}{\left(\frac{16}{3\pi}\right)^{1/4}\cdot n_w^{3/2}\cdot\int_0^\infty n^{1/2}P(n)dn}. \tag{11}$$

From eqs. (11) and (8), eliminating $F(\dot{\gamma})$,

$$\theta(\dot{\gamma},n) = \frac{\eta}{\eta_0}\cdot\frac{\dot{\gamma}\tau_0}{2}\cdot\frac{1}{n_w}\left[\frac{\int_0^\infty nP(n)dn}{\int_0^\infty n^{1/2}P(n)dn}\right]n^{1/2} = G(\dot{\gamma})\cdot n^{1/2}. \tag{12}$$

Using eq. (12) for θ, $h(\theta)$ and $g(\theta)$ can be evaluated from eqs. (1) and (2) and substituted* into eq. (6):

$$\frac{\eta}{\eta_0}G(\dot{\gamma})^{3/2} = \left(\frac{4}{\pi}\right)^{3/2}\cdot\frac{16}{3\pi}\cdot\frac{\int_0^\infty n^{1/2}P(n)dn}{\int_0^\infty n^2P(n)dn}\cdot\frac{\int_0^\infty n^{9/4}P(n)dn}{\int_0^\infty n^{7/2}P(n)dn}\cdot\frac{\int_0^\infty nP(n)dn}{\int_0^\infty n^{1/2}P(n)dn} \tag{13}$$

or

$$\frac{\eta}{\eta_0}\cdot[G(\dot{\gamma})]^{3/2} = \left(\frac{4}{\pi}\right)^{3/2}\cdot\frac{16}{3\pi}\cdot\frac{1}{n_w}\cdot\frac{\int_0^\infty n^{9/4}P(n)dn}{\int_0^\infty n^{7/2}P(n)dn}. \tag{14}$$

Finally, substituting for $G(\dot{\gamma})$ from (12) gives

$$\left(\frac{\eta}{\eta_0}\right)^{11/2}\left(\frac{\dot{\gamma}\tau_0}{2}\right)^{3/2} = \left(\frac{4}{\pi}\right)^{3/2}\cdot\frac{16}{3\pi}\cdot n_w^{7/2}\left[\frac{\int_0^\infty n^{1/2}P(n)dn}{\int_0^\infty nP(n)dn}\right]^{3/2}\cdot\frac{\int_0^\infty n^{9/2}P(n)dn}{\int_0^\infty n^{7/2}P(n)dn}. \tag{15}$$

This is the equation of the line of limiting slope. Thus, regardless of polydispersity effects, the limiting slope is $-9/11$.

The authors are grateful to Dr. W. W. Graessley for supplying the computer program used in this study.

* The assumption is implicit here that both $F(\dot{\gamma})$ and $G(\dot{\gamma})$ are large enough that the large θ-condition required for eqs. (1) and (2) is not violated, regardless of the value assigned to. The assumption is required in order that the integrals may be evaluatd over the complete range of n values. In practice, n does have a lower limit, which can be made equal to 1, representing unit or monomer chain length. Both $F(\dot{\gamma})$ and $G(\dot{\gamma})$, and thus $\theta(\dot{\gamma},n)$, can then be made as large as desired by increasing $\dot{\gamma}$, provided that the limiting slope lies between 0 and -1, i.e., that the reduced shear stress $\eta/\eta_0\cdot\dot{\gamma}\tau_0/2$ always increases with increasing shear rate $\dot{\gamma}$.

References

1. W. W. Graessley, *J. Chem. Phys.*, **47**, 1942 (1967).
2. W. W. Graessley and L. Segal, *A.I.Ch.E. J.*, **16**, 261, (1970).
3. S. Middleman, *J. Appl. Polym. Sci.*, **11**, 417 (1967).
4. G. Kraus and J. T. Gruver, *Trans. Soc. Rheol.*, **13**, 315 (1968).
5. T. W. Bates, *Eur. Polym. J.*, **8**, 19 (1972).
6. N. Nakajima and P. S. L. Wong, *Trans. Soc. Rheol.*, **9**, 3 (1965).
7. R. N. Shroff and M. Shida, *Polym. Eng. Sci.*, **11**, 200 (1971).
8. R. Sabia, *J. Appl. Polym. Sci.*, **7**, 347 (1963).
9. H. Leaderman, R. G. Smith, and L. C. Williams, *J. Polym. Sci.*, **36**, 233 (1959).
10. T. Kataoka, *J. Polym. Sci.*, **B5**, 1063 (1967).
11. J. P. Tordella, *J. Polym. Sci.*, **7**, 215 (1963).

Received September 29, 1972